A LASER HEATER FOR FERMI@ELETTRA

S.Spampinati, S. Di Mitri, B Diviacco, Sincrotrone Trieste, Italy.

Abstract

To cure the microbunching instability in the FERMI@elettra FEL a laser heater is proposed. The one-dimensional model of the instability predicts a large energy modulation cumulating as the electron beam travels along the linac. According to analytical studies and simulations the longitudinal Landau damping provided by the laser heater is expected to help in suppressing the formation of such a modulation. The efficiency of the beam heating is studied as function of the transverse laser-electron beam mismatch in the laser heater undulator in case of a realistic transverse beam profile.

INTRODUCTION

The FERMI@elettra [1] project will upgrade the Elettra linac with the installation of a photoinjector, a laser heater, an X-band cavity and two magnetic bunch compressors. The linac will then be able to provide the high current, low emittance and low energy spread (high brightness) electron beam needed by the single-pass Free Electron Laser (FEL). In this paper we describe the laser heater.

LASER HEATER

The laser heater is planned to be installed in the linac at a point where the electron beam energy is roughly 100 MeV. This device will provide a controlled increase of the uncorrelated energy spread. According to analytical and numerical studies, the beam heating is expected to help in suppressing the microbunching instability through longitudinal Landau damping [2].

The laser heater layout is shown in Figure 1.

The laser heater consists of an undulator located within a small magnetic chicane that allows an external laser to seed the electron beam. There is space for further diagnostic devices beyond the exit of the laser heater undulator.
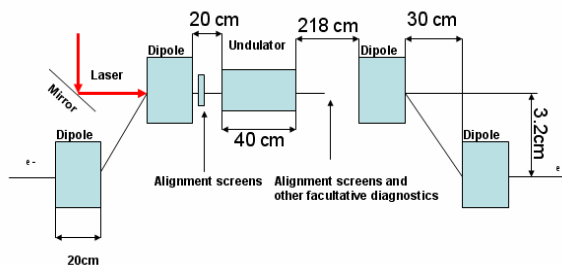

Figure 1: Schematic of the laser heater layout.

The particles interact with the laser in the short undulator and they gain an energy modulation with a periodicity on the scale of the optical wavelength. The

corresponding density modulation is negligible; however, the induced energy/position correlation is smeared by the transverse motion in the chicane. As a result, the laser/electron interaction leads to an effective heating of the beam. The main laser heater parameters are listed in the Table 1.

The laser used for the heater will be split from the main beam of the Ti:Sa laser used for the photoinjector laser system. The maximum peak laser power available in the undulator is 10 MW. The IR laser will be stretched to reach a pulse duration of 20 ps. The pulse energy needed is <1mJ, therefore only a small part of the infrared light energy available (for laser heater and photocathode, >18mJ) will be needed for the laser heater. The induced energy spread must be in the rage 10 – 20 keV RMS [3].

Table 1: Mean laser heater parameters

Parameter	value
Undulator period	4 cm
Number of periods	12
Bending angle	3.5 degrees
Bending length	20 cm
Drift between bending	30 cm
Drift before undulator	20 cm
Drift after undulator	218 cm
Total length	418 cm

Neglecting changes in the laser and beam transverse dimensions during the interaction, the provided energy modulation for a "hard edge" undulator filed [4] is given by equation.(1):

$$\Delta\gamma_L(r) = \sqrt{\frac{P_L}{P_0}}\,\frac{K\,L_U}{\gamma_0\,\sigma_r}\left[J_0\left(\frac{K^2}{4+2K^2}\right) - J_1\left(\frac{K^2}{4+2K^2}\right)\right]\cdot e^{-\frac{r^2}{4\sigma_r^2}}\frac{\sin(\frac{\nu_0}{2})}{\frac{\nu_0}{2}}$$

with:

$$\nu_0 = 2\pi N\frac{(\lambda - \lambda_r)}{\lambda} \quad (2)$$

P_L is the laser peak power, $P_0 = 8.7GW$, r is the average radius of the electron beam transverse size, σ_r is the RMS laser spot size in the undulator and $\gamma_0 mc^2$ is the average total energy of the electron beam. J_0 and J_1 are the Bessel functions, K is the undulator parameter, L_u is the undulator length, λ_u is the undulator period, N is the number of periods of the

undulator, I is the laser intensity, γ is the Lorentz factor, λ_r is the resonance wavelength of the laser/electron interaction and λ is the laser wavelength.

The ratio R between the energy modulation $\Delta\gamma_L$ and the energy spread σ_γ depends on the transverse parameter B defined as:

$$B = \frac{\sigma_r}{\sigma_x} \qquad (3)$$

where σ_x is the rms horizontal size of the electron beam.

R is 2 for B=1 and it is <2 for B>1. As the Landau damping is less effective for B<1, it is possible to estimate the needed laser power by using R=2 that is:

$$\sigma_\gamma = \frac{\Delta\gamma_L(0)}{2} \qquad (4)$$

UNDULATOR

The laser heater undulator is a simple planar permanent magnetic structure. It is designed to be resonant at the 780 nm nominal wavelength of the Ti:Sa photocathode laser for an average beam energy ranging from 85 MeV to 105 MeV. The resonant condition is:

$$\lambda_0 = \frac{\lambda_u}{2\gamma^2}\left(1 + \frac{K^2}{2}\right) \qquad (5)$$

The undulator period determines the minimum energy at which the undulator is resonant and the minimum gap needed. The undulator is not resonant at a beam energy of 85 MeV for a periods longer than 4.3 cm given the minimum gap required is too tight for a period shorter than 4.0 cm. These considerations are made explicit in Figure 2. A period 4 cm long has been therefore chosen.

The number of periods has to be limited in order to have a large energy acceptance. Figure 3 shows the variation of energy spread as a function of the laser detuning for various number of undulator periods.
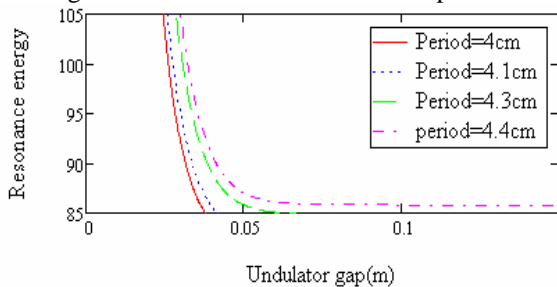

Figure 2: Resonance energy in MeV vs. undulator gap. The undulator tunability has been evaluated for different undulator period lengths.
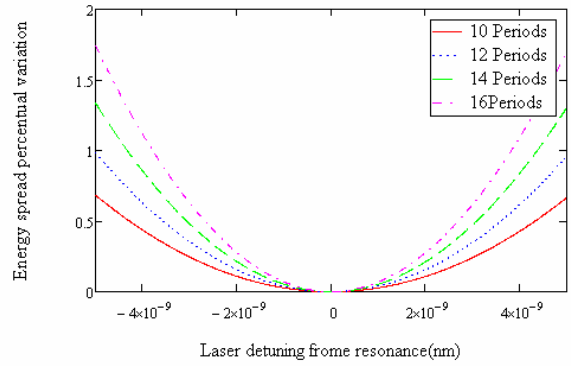

Figure 3: Energy spread percentage variation vs. laser wavelength detuning from the resonance condition.

The present undulator design includes 12 periods (8-10 effective periods) for a total length of 48 cm. The terminations are designed to have no residual dispersion and to provide no orbit displacement. The gap range is 24 – 38 mm for a maximum peak field in the range 0.312 T – 0.102 T.

According to the undulator parameters discussed so far, eq. (4) predicts a peak power of 0.5 MW to induce an energy spread of 20 keV rms.

CHICANE DYNAMICS

The effects of the laser heater chicane on the beam have been analysed. The particle longitudinal coordinate along the bunch (*i.e.*, referred to the beam centre of mass) when the beam reaches the centre of the chicane can be evaluated through the 2nd order transport matrices at the same location and the initial energy and transverse coordinates:

$$z(f) = z(i) + R_{51}x + R_{52}x' + R_{56}\frac{\delta_\gamma}{\gamma_0} + T_{566}\left(\frac{\delta_\gamma}{\gamma_0}\right)^2 \quad (6)$$

For a symmetric achromatic chicane, $R_{51} = 0\,\mathrm{m}$. The energy/position correlation induced by the interaction is smeared if the following relation is satisfied [5]:

$$|R_{52}|\sigma_{x'} > \frac{\lambda_L}{2\pi} \qquad (7)$$

For FERMI, $R_{52} = 0.031\,\mathrm{m}$, $\beta \approx 2.5\,\mathrm{m}$ and $\sigma_{x'} = \sqrt{\varepsilon_x}/\beta_x \approx 55\,\mu m$. Thus, the correlation is efficiently smeared for a finite emittance beam as shown in Figure 4.
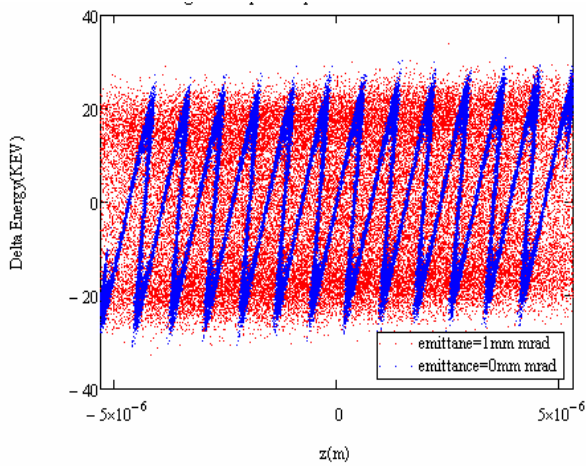
Figure 4: Longitudinal phase space (energy spread in KeV vs. bunch length in m) out of the laser heater chicane. A finite transverse normalized emittance of 1 mm mrad is sufficient to smear the energy/position correlation induced by the laser/electron interaction. For comparison, we show that the smearing effect does not happen for a null emittance, *i.e.* the correlation persists.

Exiting the photoinjector, the bunch head as at a higher energy respect to the bunch tail, therefore eq.(6) describes a beam lengthening. Given the design parameters reported in Table 1 and the known beam energy chirp provided by running off-crest in the upstream linac (the photoinjector accelerates approximately on crest), the laser heater chicane produces an increase of the beam length of about 2%. This effect is not critical for the subsequent compression.

Moreover, as the energy spread increases in the dispersive region, the heating can lead to an emittance dilution by additionally induced betatron motion. The relative emittance growth can be estimated by [5]:

$$\frac{\Delta\varepsilon_x}{\varepsilon_x} = \frac{1}{2}\left(\frac{\sigma_\gamma\eta}{\gamma_0\sigma_x}\right)^2 \qquad (8)$$

For FERMI this effect is negligible since $\frac{\Delta\varepsilon_x}{\varepsilon_x} = 1.5 \cdot 10^{-5}$

PARTICLE TRACKING

Using the tracking code elegant [x], particle tracking has been performed on a 6 dimensional Gaussian electron beam with elegant code. The energy distribution of the electron beam generated by the photo-cathode has been reproduced in elegant and is shown in Figures 5.
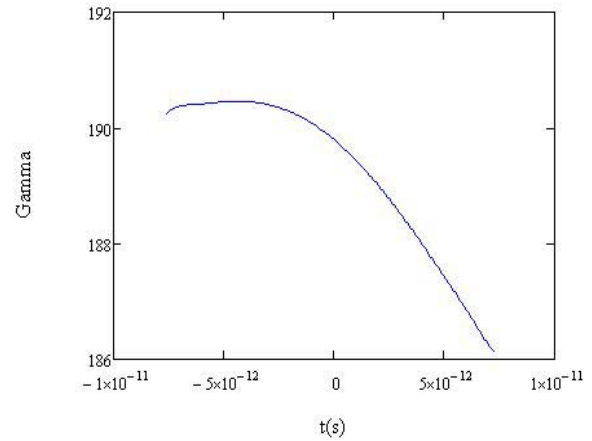

Figure 5: Energy profile of the beam out of the photo-injector.

According to the energy distribution shown in Figure 5, the dispersive motion in the laser heater chicane generates a different transverse displacement of the beam longitudinal slices with respect to the undulator axis (see, Figure 6).

The different overlap of each slice with the seeding laser, together with the variation of the slice transverse dimension also shown in Figure 6, leads to a non-uniform beam heating.
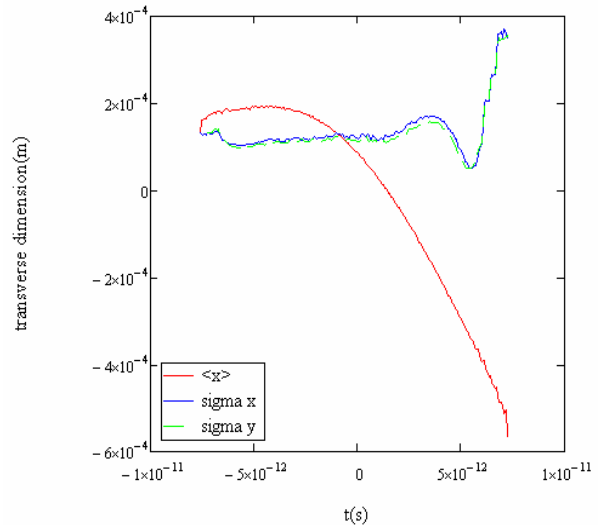

Figure 6: Mean transverse (x) position and transverse (x, y) rms dimensions of the beam in the chicane.

Different runs have been performed by changing the laser waist from 480 ☐m (B=2 for the flat part of the beam) to 240 ☐m (B=1 for the flat part of he beam) to obtain a more uniform beam heating. Accordingly, the laser power has been changed (see, eq.(1)) to induce always the same uncorrelated energy spread. Results are shown in Figures 7 and 8.
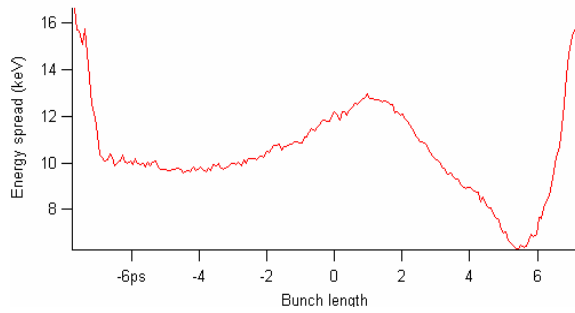
Figure 7: Rms uncorrelated energy spread along the bunch. Laser waist is 240 □m (B=1 for the flat part of the beam). Laser peak power is 0.130 MW.
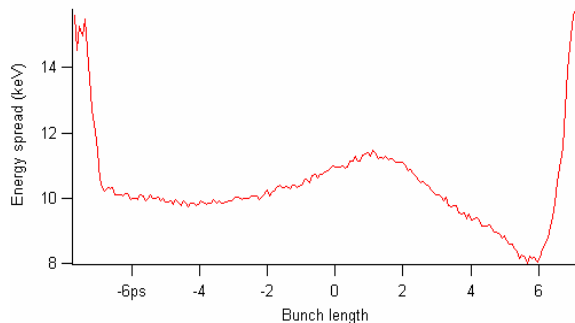

Figure 8: Rms uncorrelated energy spread along the bunch. Laser waist is 480 □m (B=2 for the flat part of the beam). Laser peak power is 0.165 MW.

The resulting beam was then propagated through the rest of the linac. The longitudinal phase space at the end of the linac is shown in Figure 9 and in Figure 10, corresponding to Figure 7 and Figure 8, respectively.
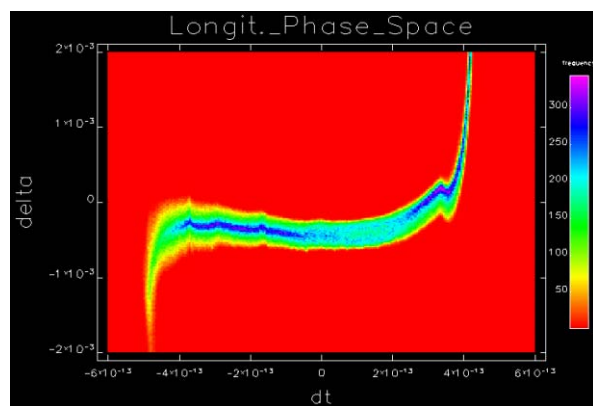

Figure 9: Longitudinal phase space (relative energy spread vs. bunch duration) at the linac end, corresponding to the beam heating in Figure 7.
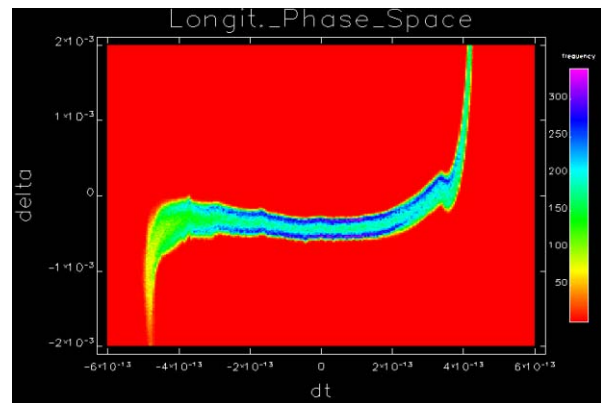

Figure 10: Longitudinal phase space (relative energy spread vs. bunch duration) at the linac end, corresponding to the beam heating in Figure 8.

Simulations predict that an rms uncorrelated energy spread of 10 keV can be induced uniformly over about 60% of the bunch duration with a laser waist of 480 □m and a peak power of 0.165 MW. Preliminary calculations indicate that 37 keV energy spread can be reached in the bunch core with a the maximum peak power of 10 MW at a beam energy of 85 MeV.

CONCLUSIONS

The parameters of the laser heater main components (undulator and magnetic chicane) have been explored. Analytical calculations and particle tracking demonstrate that the peak power by the Ti:Sa photocathode laser is sufficient for the required beam heating.

[1] FERMI@elettra CDR, to be published.
[2] E.L. Saldin, E.A. Schnaidmiller, M.V. Yurkov, Nuclear Instruments and Methods A 429 (1999) 233.
[3] A.Zolents et al., Fermi Tecnical Note 06/15 (2006).
[4] G.Dattoli, A.Renieri, Laser Handbook Vol.4 (1984).
[5] Z.Huang et al., Phys Rev ST-AB **7** 074401 (2004).
[6] M.Borland, APS LS-287 (2000).